CURRENT-DRIVE EXPERIMENTS ON THE PLT TOKAMAK

By

F. Jobes, S. Bernabei, P. Efthimion, W. Hooke, J. Hosea,
E. Mazzucato, E. Meservey, R. Motley, J. Stevens,
and S. von Goeler

JUNE 1983

PLASMA
PHYSICS
LABORATORY

PRINCETON UNIVERSITY
PRINCETON, NEW JERSEY

CURRENT-DRIVE EXPERIMENTS ON THE PLT TOKAMAK

F. Jobes, S. Bernabei, P. Efthimion, W. Hooke, J. Hosea,

E. Mazzucato, E. Meservey, R. Motley, J. Stevens,

and S. von Goeler

Plasma Physics Laboratory, Princeton University

Princeton, New Jersey 08544

ABSTRACT

Lower hybrid current-drive experiments have been carried out c the PLT

Tokamak. Steady currents up to 175 kA have been maintained for three seconds

and 400 kA for 0.3 sec by the rf power alone. The principal current carrier

appears to be a high-energy ($\sim$ 100-keV) electron tail, concentrated in the

central 20-40 cm diameter core of the 80-cm PLT discharge. Effective current

drive is observed only for $\bar{n}_e < 8 \times 10^{12}$ cm^{-3}. This limitation may be a wave-

propagation phenomenon and not a fundamental plasma-physics effect.

DISCLAIMER

MASTER

I.   INTRODUCTION

Lower hybrid experiments have been carried out on the PLT Tokamak (major radius 1.3 m and minor radius 0.4 m),[1] and up to 500 kW of power at 800 MHz has been delivered to the plasma by means of a radiating antenna consisting of a six-element stainless steel waveguide grill.[2] Each waveguide, measuring 22 cm x 3.5 cm, is driven by a klystron with independent adjustment for power and phase, as shown schematically in Fig. 1.   The phase control allows us to vary the $n_{\parallel}$-spectrum up to a maximum of $n_{\parallel} = 4.5$ and to launch the waves in one preferred direction, i.e., co or counter to the plasma current.   Coupling into the plasma load is excellent, with reflection typically 10-20% and is in very good agreement with linear theory.[3] Steady currents up to 175 kA have been maintained for three seconds and 400 kA for 0.3 seconds by the rf power alone.   The principal current carrier appears to be a high energy ($\sim$ 100 keV) electron tail concentrated in the central 20-40 cm diameter core of the 80 cm PLT plasma.   Effective current drive is observed only for $\bar{n}_e \lesssim 8 \times 10^{12}$ cm-3.

II.   EXPERIMENTAL PROCEDURE

In this experiment, the discharge is initiated in the normal fashion using the ohmic heating transformer, but the external inductive power is turned off (by holding the primary current constant) starting about 200 msec after breakdown.   Occasionally the primary current is turned completely off instead of being held constant.   The population of superthermal electrons in the target plasma is kept as low as possible by imposing a small initial loop voltage and by bringing the density up to about 8-10 x 10^{12} cm^{-3} before it is reduced to the level used for the current drive -- typically 2 to 8 x 10^{12} cm^{-3}.   This early density rise serves to decrease the number of run-away electrons when the plasma is initiated.

The plasma current is initially 300-400 kA and typically decays about 100 kA before the rf is applied. This initial decay is approximately exponential; however, after the rf is applied, the rate of change of the current is approximately constant. With sufficient power, the current can be made constant or even increased. The rf pulse is sufficiently long to allow the current radial distribution to reach an equilibrium so that the effects of internal inductance variations are negligible. However, it often takes 300 ms or longer to reach the final steady state. The pulse durations in these experiments are limited by heating in the rf equipment and not by any plasma related phenomena.

Figure 2 is an example of this procedure. In this case the rf was left on for longer than the computerized data taking, and so the end of the discharge is not recorded. The OH primary current is held constant at ~ 2.2 kA after 300 msec, and the rf, which comes on at 200 msec is sufficient to maintain the current with a very slight increase. The internal inductance settles very quickly after the rf comes on and then increases slightly.

Long pulse operation is shown in Fig. 3. Current and density are displayed for three different shots, in which the rf was on for 0, 2 and 3.5 seconds, starting at 0.4 sec. The effect of the rf was to delay completely the decay of the current until the end of the rf. In the 3.5 sec case, the equilibrium field was turned off immediately after the end of the rf, thus abruptly terminating the discharge. It appears from Fig. 3 that, rf circuitry permitting, the tokamak pulse could be extended indefinitely.

Plasma currents of up to 400 kA have been driven for 300 msec, and as shown in Fig. 4, the plasma current can also be made to increase.

III.   POWER FLOW MEASUREMENTS

The power flow equation for the tokamak current can be written as:

$$\eta P_{RF} + P_{ext} = I^2 R + \frac{d}{dt} (I^2 L/2) \quad . \tag{1}$$

Here ηP_{RF} is the rf power driving the electrons and, in equilibrium, is the collisional power dissipated by these electrons, P_{ext} is the power dissipated by these electrons, P_{ext} is the power flowing into the plasma from the tokamak equilibrium field coils, $I^2 R$ is the collisional dissipation of the rf driven current and $I^2 L/2$ is the total inductive energy of the plasma current.

All of the quantities in Eq. 1 can be measured experimentally with the exception of η, the efficiency, and R.   In practice, we can make our measurements during the time the rf is on and after the rf is turned off. Under the assumption that R immediately before and after the rf turn-off is constant, we have, in effect, two equations in two unknowns.

In his 1978 paper Fisch[4] gives formulae giving the ratio of dissipation power to plasma current expressed in terms of the plasma and wave parameters.   In terms of the parameters here, this ratio, in equilibrium is

$$\frac{\eta P_{RF}}{1} = IR \equiv V_d \tag{2}$$

where V_d has the dimensions of volts and corresponds physically to the energy lost through collisions by the fast electrons in one turn around the torus.

In order to compare the experimental observations with the theory, we identify the quantity V_d above with the ratio $P/_I$ which is computed by Fisch.   In Fig. 5, for example, we plot V_d vs. density.   The line is a rough fit to the data.   The slope of the line is about 2 to 3 times greater than the

theoretical value from Karney and Fisch[5] for Z_{eff} = 5. The Z_{eff} in these low density discharges has not been measured directly, but indirect estimates indicate that Z_{eff} is in this range. The theoretical value itself could vary by a factor of two or even more, however, depending upon the assumptions made about the rf spectrum in the core of the plasma and the containment time of the tail electorns. Relativistic effects (which are ignored here) would also increase the slope.

The theory does not explain the sharp density limit at $\sim 8 \times 10^{12}$ cm^{-3}, nor does it explain the mechanism by which the superthermals are generated in a relatively cold ($\sim$ 800 eV) plasma. However, the rough agreement with the above very simple plasma model indicates that the steady-state current drive we see is very closely related to the theory involving collisions between lower hybrid waves and plasma electrons.

Figure 6 is a plot of the efficiency, η, as a function of density corresponding to the data of Fig. 5. It should be noted that at densities at which V_d falls below predicted values, the efficiencies are quite low.

IV. SUPERTHERMAL ELECTRONS

Besides the gross behavior of the plasma there is other ample evidence that there is a large population of superthermal electrons. This evidence is found in both unusual synchrotron radiation signals and in numerous X-ray studies. The synchrotron radiation is shown in Fig. 7. The amplitude of the signals emitted at various frequencies takes a sudden jump when the rf is turned on. The frequencies are here expressed in terms of the radius at which that frequency equals the electron cyclotron frequency (for low energy thermal electrons) and the amplitudes are calibrated in terms of blackbody electron temperatures. (Since the plasma is not a blackbody at these densities, these

signals do not represent true electron temperatures.) The signal at 191 cm is of special interest, because that (major) radius lies outside the vacuum vessel. That signal must have been doppler-shifted, and, indeed, if the signal originated in the center of the plasma column, then the electrons must have been streaming at energies of between 50 and 200 keV. The bottom trace in Fig. 7 is emission at the second harmonic of the electron cyclotron frequency. This radiation is not sensitive to parallel streaming; its slow growth would indicate a gradual build-up of electrons with high perpendicular energies.

The X-ray evidence for superthermal electrons can be seen in Figs. 8, 9 and 10. Figure 8a shows an X-ray spectrum before the rf is turned on. It shows an exponential fall-off with energy which matches the approximately 1 keV Thomson-scattering temperature measurements which are insensitive to a high energy tail. (The plasma conditions are shown in Fig. 2.) After the rf is turned on, on the other hand, there is indeed a tail, as shown in Fig. 8b. This tail lasts for the duration of the rf and for a few hundred msecs afterward. The spectra taken at different times during rf are virtually identical. The tail is also shown in Fig. 9, on a much larger energy scale. Figure 9 is a relatively high density case - 6×10^{12} cm^{-3}. The current was held constant in this case, so that there was no E-field to drive the electrons up to high energies. The tail spectra of lower density cases are about the same, both in amplitude and in tail "temperature," about 50 keV. Also shown is the X-ray signal from a similar plasma shot in which there was no rf current drive. No rf shots differ fundamentally from the current drive shots in that there is a finite dI/dt which provides an E-field which could drive run-away electrons to very high energies. In these non-rf cases at the higher densities there were essentially no X rays in the tail region, but at lower densities there were many.

Further evidence concerning the superthermal electrons comes from the spatial distribution of the X-ray emission, shown in Fig. 10. This graph shows the radial variation of 14 keV X-ray intensity after Abel inversion for three different plasma conditions; q(a) decreases from case A to case C. The X-ray profiles can be seen to broaden in a fashion similar to what one would expect of the current profile.

So far, all the X-ray measurements have been perpendicular to the magnetic field; we have no direct evidence that the electrons are a beam. However, the X-ray intensity is lower than we expect for a nearly isotropic high energy electron distribution with a sufficent number of electrons to carry all the plasma current. On the other hand, the intensity is about right if the electrons are in a beam.

V.   HIGH DENSITY LIMIT

At high densities ($n_e > 8 \times 10^{12}$ cm^{-3}) the current drive seems to disappear. Unlike the lower density cases there is no observable effect of the rf power. In part, this problem is caused by the dissipation factor, V_d, which increases in proportion to density. At higher density more power is needed, and with a fixed power less current can be driven. However, this is not all of the problem. Figure 6 shows that the efficiency η falls off sharply at these higher densities. The efficiencies are shown again in Fig. 11, plotted as a function of the ratio of the lower hybrid frequency to the driving frequency (the lower hybrid frequency is calculated using the line average density). We have an indication here that the high density limit may be a wave propagation problem and not a density problem because the efficiency falls off as the lower hybrid frequency approaches one-half the driving frequency, which is where one would expect parametric decay, ion interactions, and shifts in the $n_{\parallel}$ spectrum to become important competing effects.

Another indication that the density limit may be cause by wave problems is shown in Fig. 12 which is two wave spectra picked up by an antenna in the PLT control room. These spectra are essentially identical to spectra picked up on Langmuir probes in the plasma periphery. The low density case shows only the 800 MHz rf signal (plus some pickup from commercial TV stations), but the high density (9×10^{12} cm^{-3}) case has a very rich spectrum. The power in these sideband frequencies increases dramatically with density. This radiation is very likely scattered by plasma turbulence which could well be the cause of the reduced efficiencies at higher densities.

REFERENCES

[1]D. Grove et al., Conf. on Plasma Physics and Nuclear Fusion Research, Vol. I., p. 21 (IAEA, Vienna, 1977).

[2]P. Lallia, Proc. of 2nd Topical Conference on rf Plasma Heating, Lubbock, Texas, (1974) Texas Tec. University, Lubbock, Texas.

[3]M. Brambialla, Nucl. Fusion 16, 47 (1976).

[4]N. J. Fisch, Phys. Rev. Lett. 41, 873 (1978).

[5]C.F.F. Karney, and N.J. Fisch, Phys. Fluids 22, 1 ., (1979).

FIGURE CAPTIONS

FIG. 1   A schematic diagram of PLT and the lower hybrid apparatus.

FIG. 2   The waveforms of important plasma parameters in an rf current-drive
discharge. The rf drive extended to 1000 msec.

FIG. 3   Current and density waveforms for 3 discharges, with rf lasting 0,
2 and 3.5 seconds, starting at 0.4 sec. The density scale is 1 x
10^{13} per major division. In the 3.5 second case, the discharge was
terminated at 3.9 sec, 0.1 sec after the end of the rf pulse. The
rf power was 100 kW.

FIG. 4   Current and voltage waveforms for a discharge in which the current
was made to increase. The net rf power was 370 kW and it was on
from 300 to 500 msec.

FIG. 5   The ratio of dissipation power [calculated just after rf shut-off
from $d/dt \ (1/2 \ LI^2) = I^2R$] to plasma current as a function of
density for a variety of discharges. The ratio is a voltage. The
line is a rough fit to the data.

FIG. 6   The efficiency of the rf drive as a function of density. This
efficiency is the ratio of power required to drive the current, as
measured after the rf pulse, to the rf power.

FIG. 7   Ordinary mode radiation near the electron cyclotron frequency for
          an rf driven current. The rf is on from 250 to 750 msec. The
          amplitudes of the signals are calibrated in terms of blackbody
          electron temperatures; however, the plasma density was too low in
          the case for the radiation to be blackbody. The values of major
          radius corresponds to une location of resonance field in the
          absence of any Doppler shift.

FIG. 8   Plasma X-ray spectra in the 1 to 25 keV energy range. Before rf
          (top) and after rf (bottom). The temperature shown in each graph
          refers to the slope of the line shown through the points.

FIG. 9   Plasma X-ray spectrum from NaI detector. $B_t \approx 31$ kG, $I_p = 200$ kA,
          $P_{RF} = 200$ kW, $\bar{n}_e = 6 \times 10^{12}$ cm^{-3}.

FIG. 10   Radial variation of X-ray intensity at 14 keV from a moveable
          silicon detector, after Abel inversion, $\bar{n}_e = 5 \times 10^{12}$ cm^{-3}. A:
          $P_{RF} = 200$ kW, $I_p = 200$ kA, $B_t = 31$ kG; B: $P_{RF} = 250$ kW, $I_p = 210$
          kA, $B_t = 15.7$; C: $P_{RF} = 320$ KW, $I_p = 290$ kA, $B_t = 15$ kG.

FIG. 11   Efficiencies of rf current drive as a function of the ratio of the
          lower hybrid frequency, calculated from the line average density,
          to the driving frequency. The efficiencies are the same as in Fig.
          6.

FIG. 12   RF spectra picked up by an antenna near the PLT device for

discharges at densities of 9 (top) and 3 (bottom) x 10^{12} cm^3.

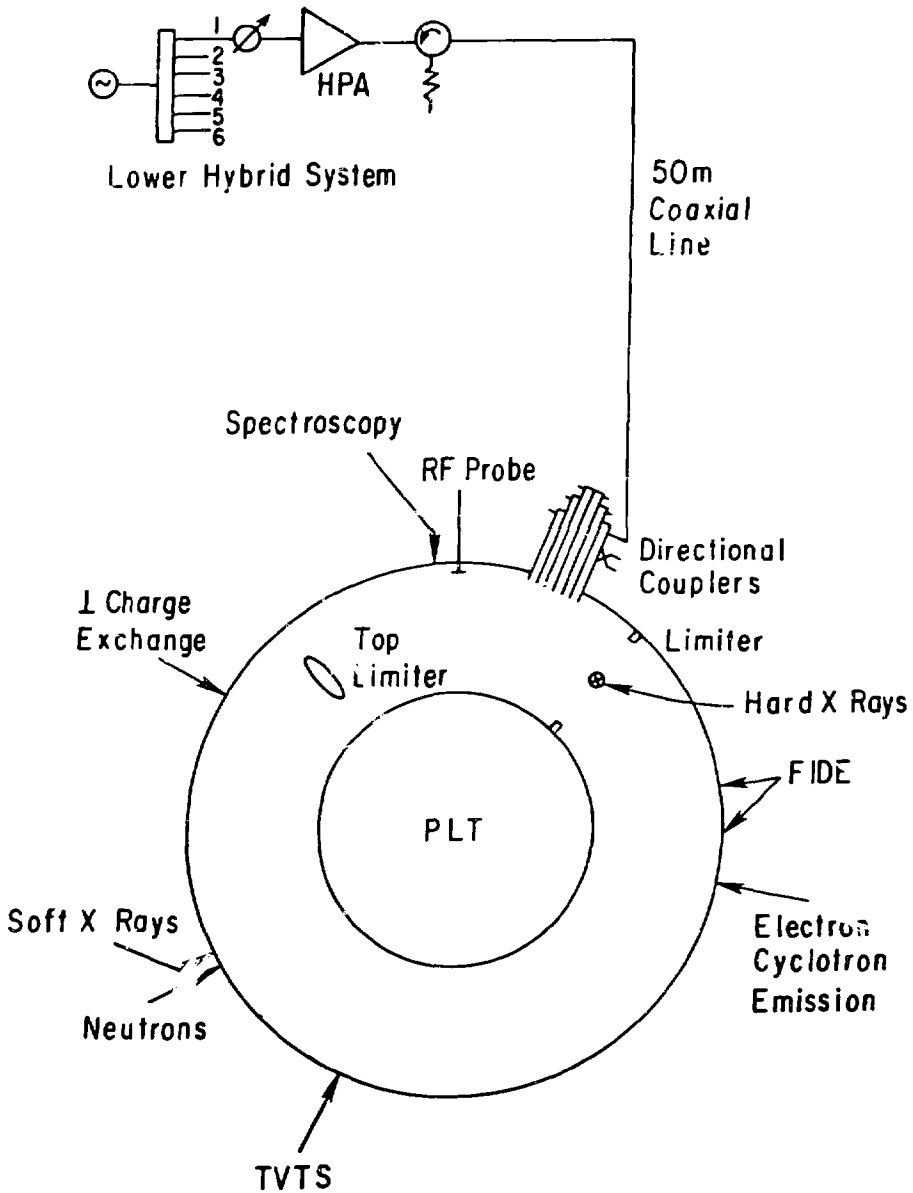These spectra are similar to those picked up by Langmiur probes in
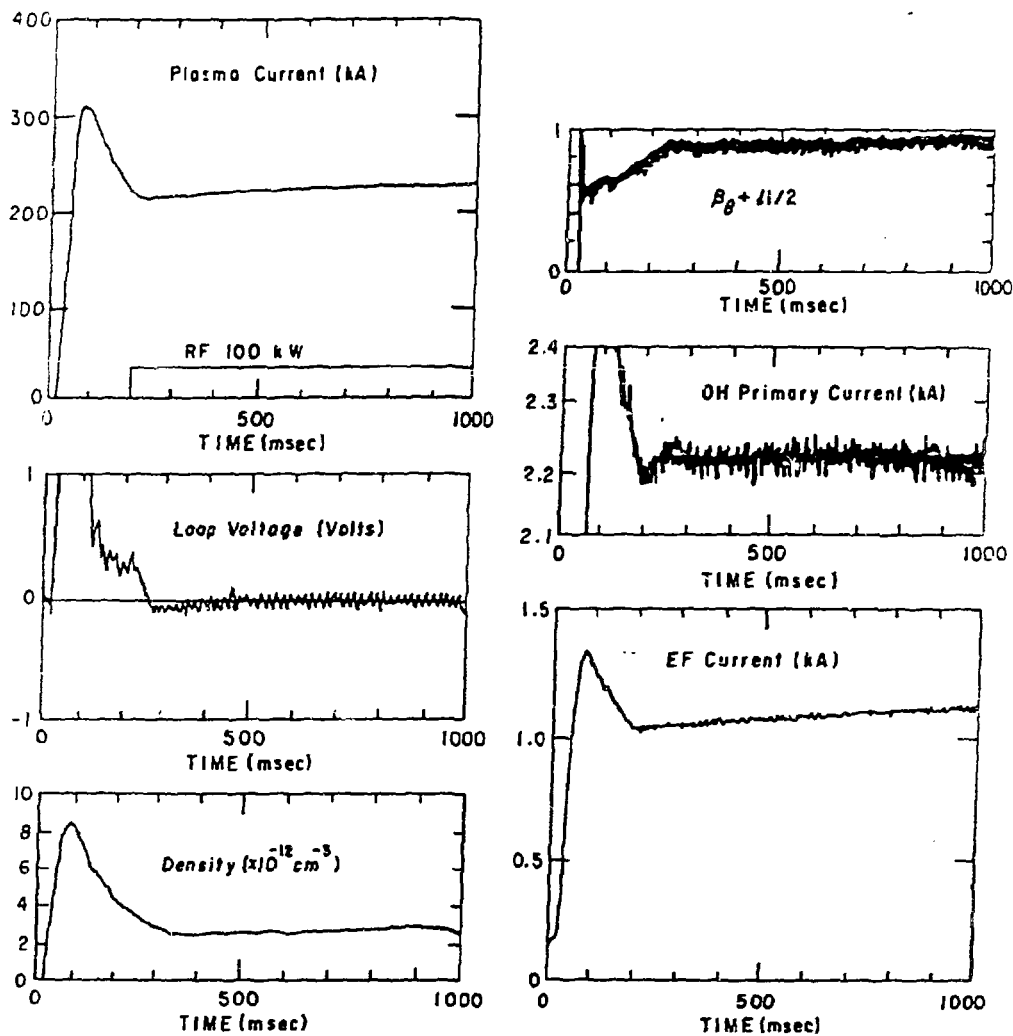
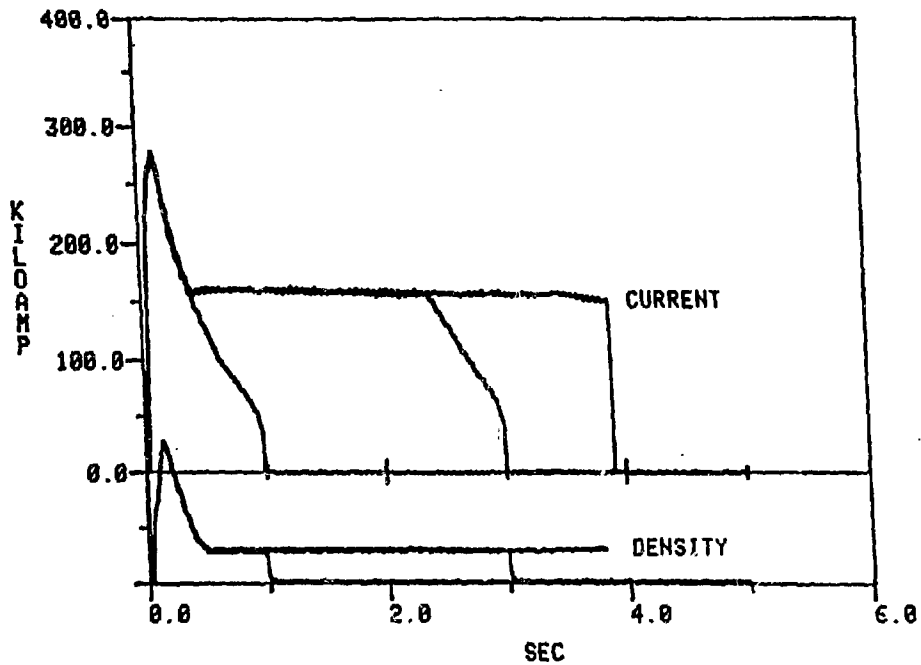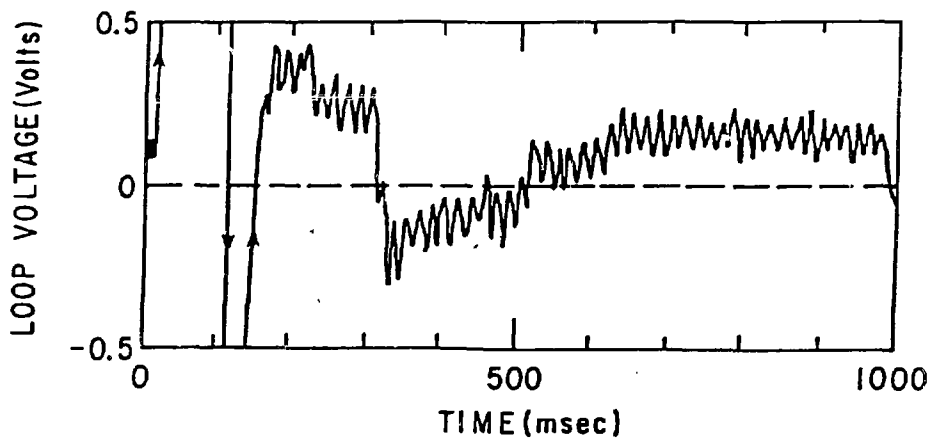the plasma periphery.

#82X0165

Fig. 1

Fig. 2

Fig. 3

#82X0161

Fig. 4

V-LOSS VS DENSITY

DENSITY (10^{12})
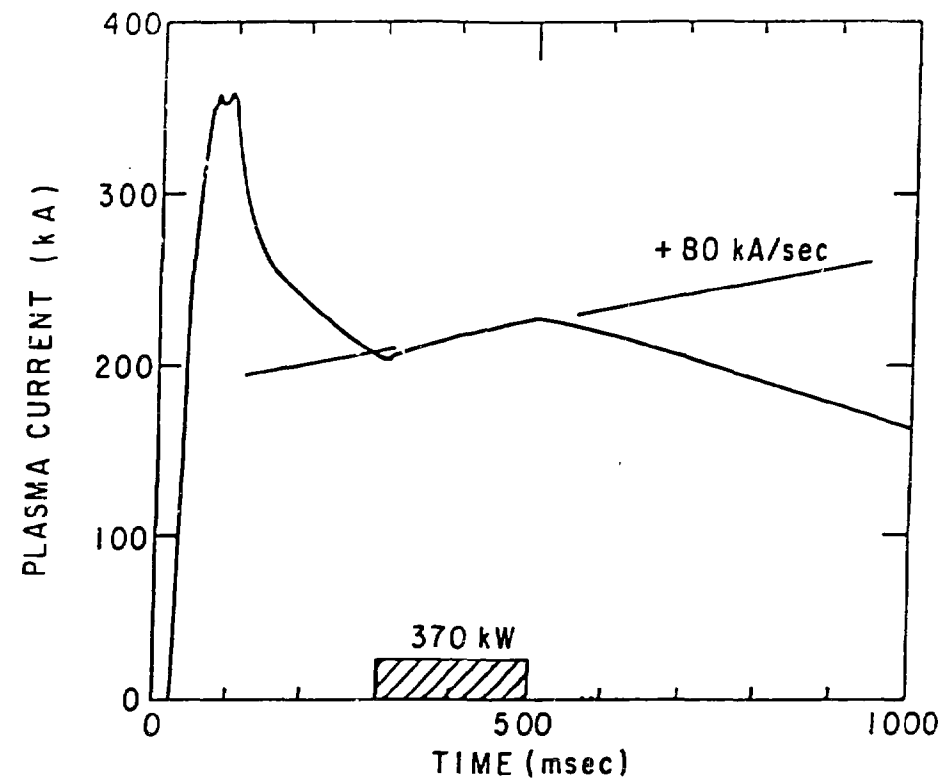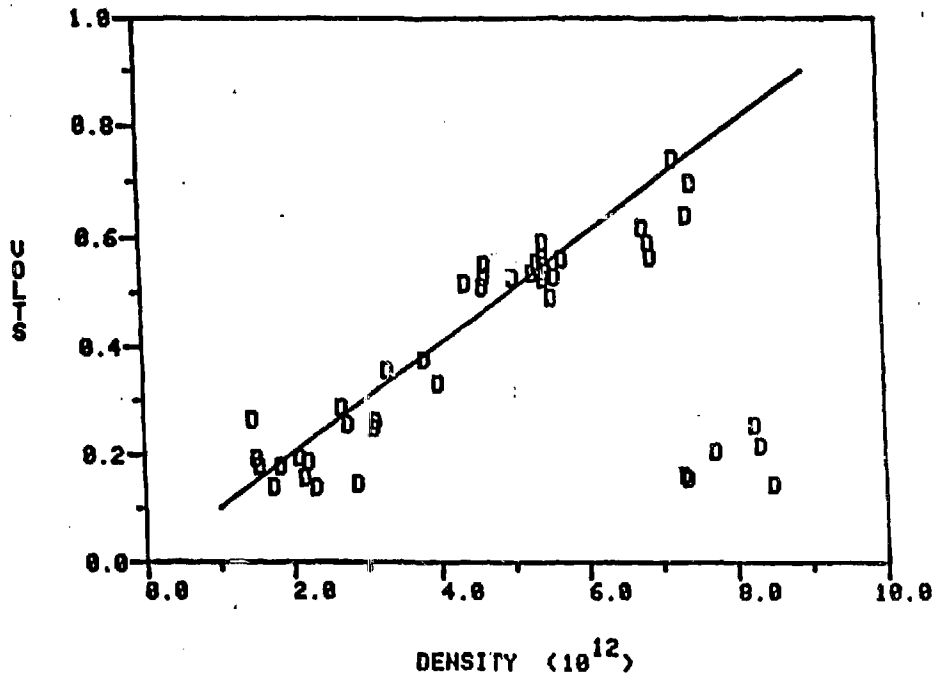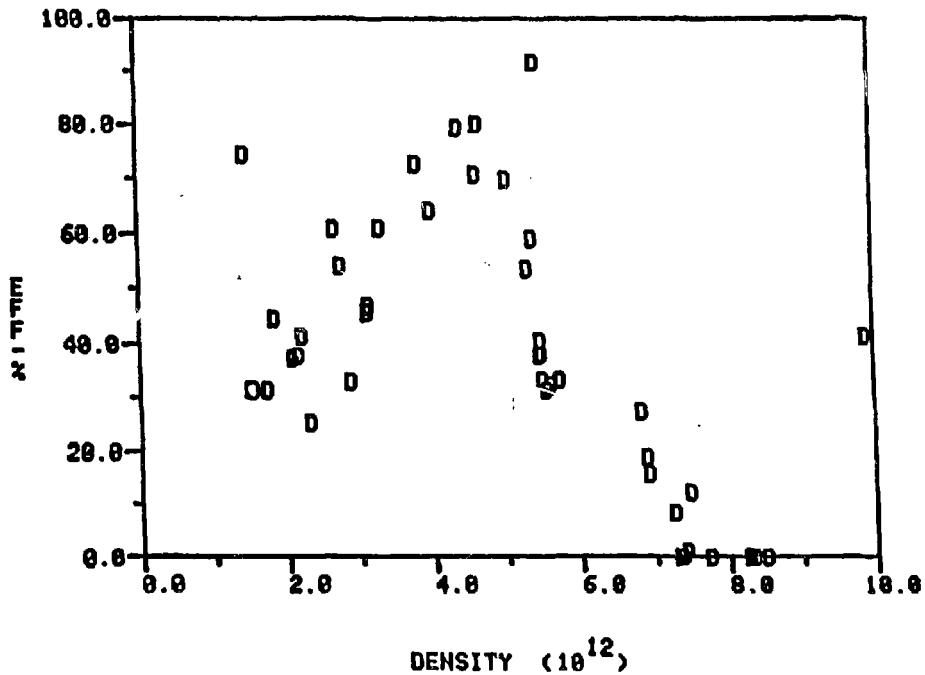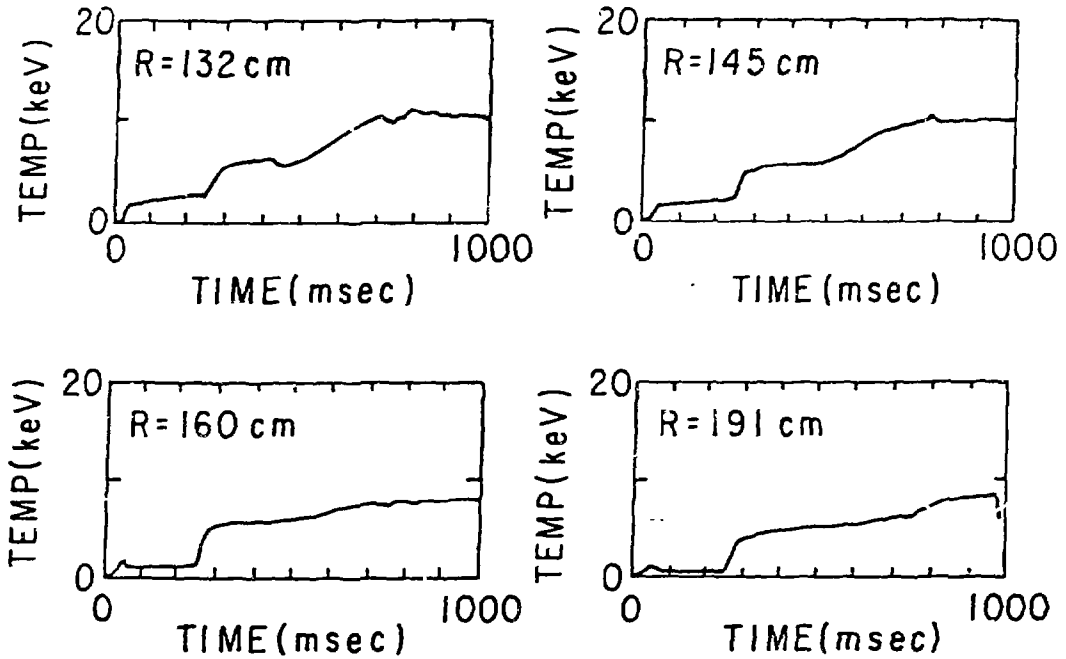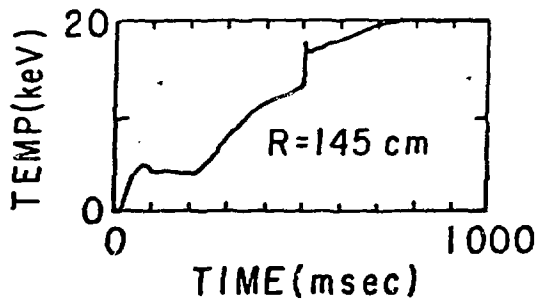
Fig. 5

EFF-% VS DENSITY

Fig. 6

#81X1315

ORDINARY MODE ECE $\omega = \Omega_{ce}$

EXTRAORDINARY MODE ECE $\omega = 2\Omega_{ce}$

Fig. 7
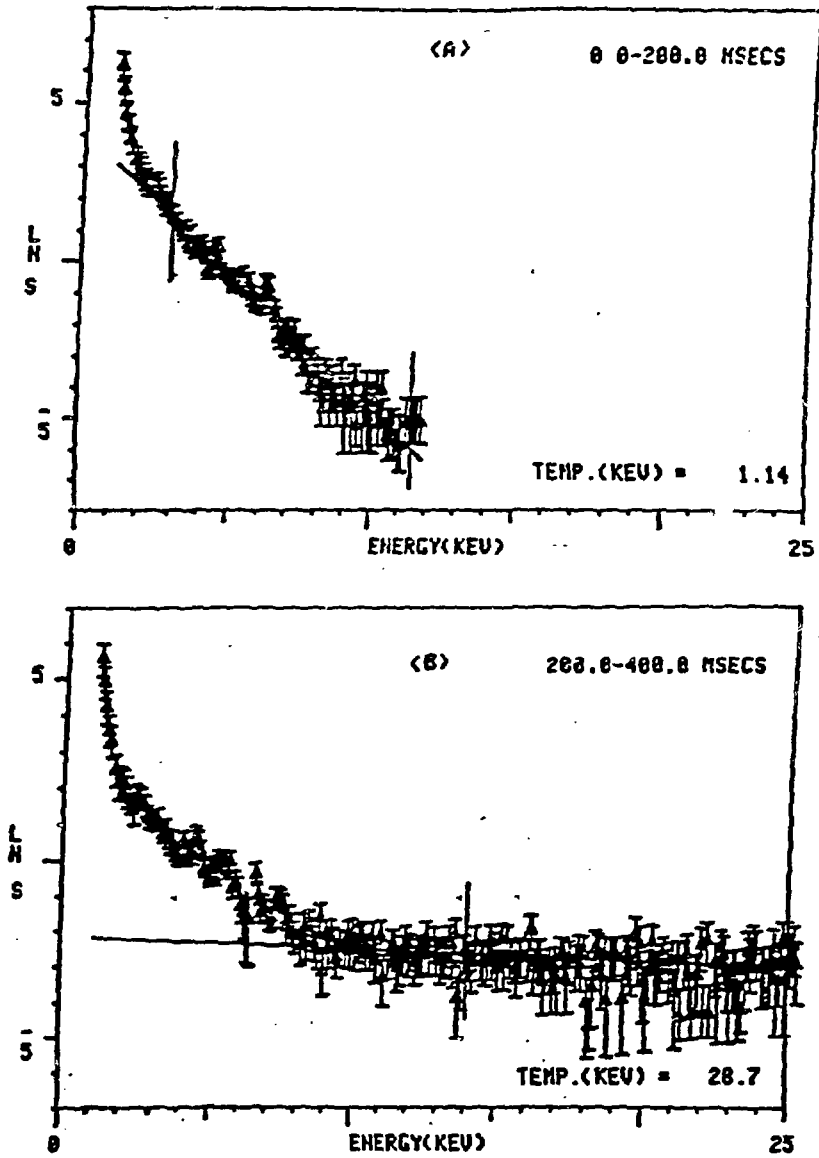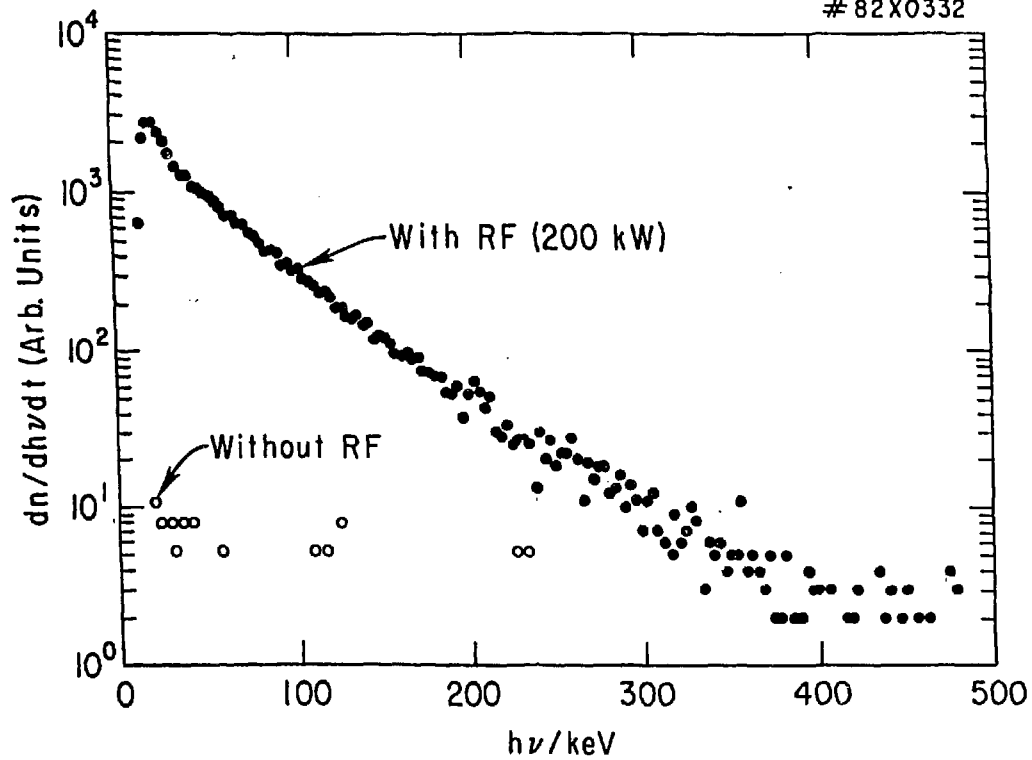
Fig. 8

Fig. 9
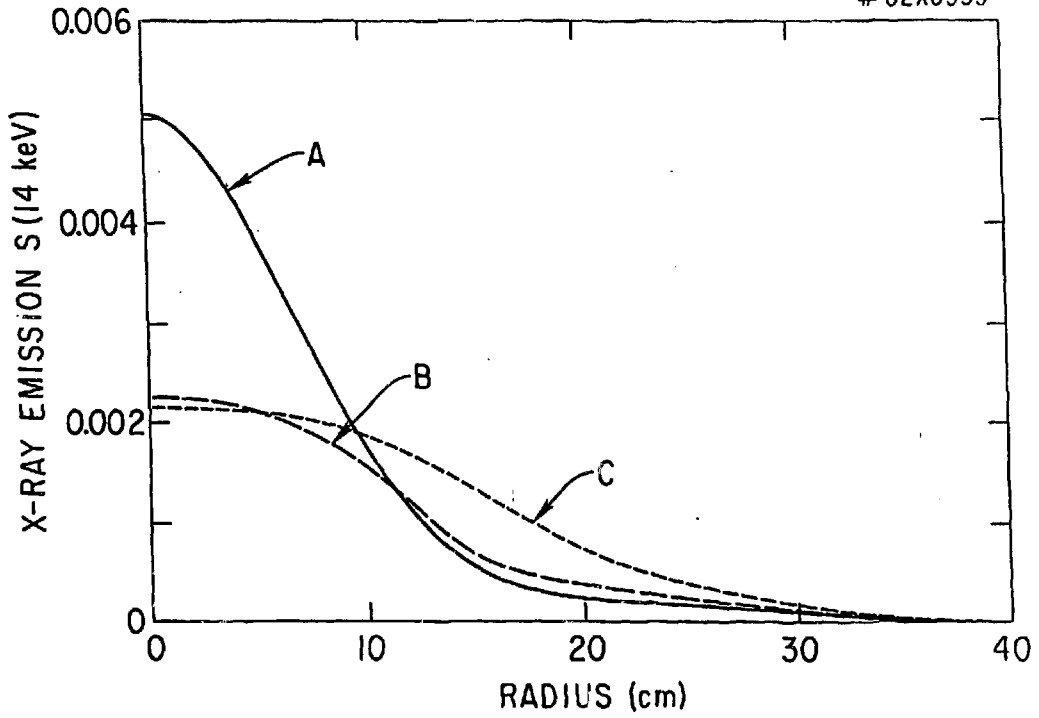
Fig. 10

EFF-% VS OMEGA-LH
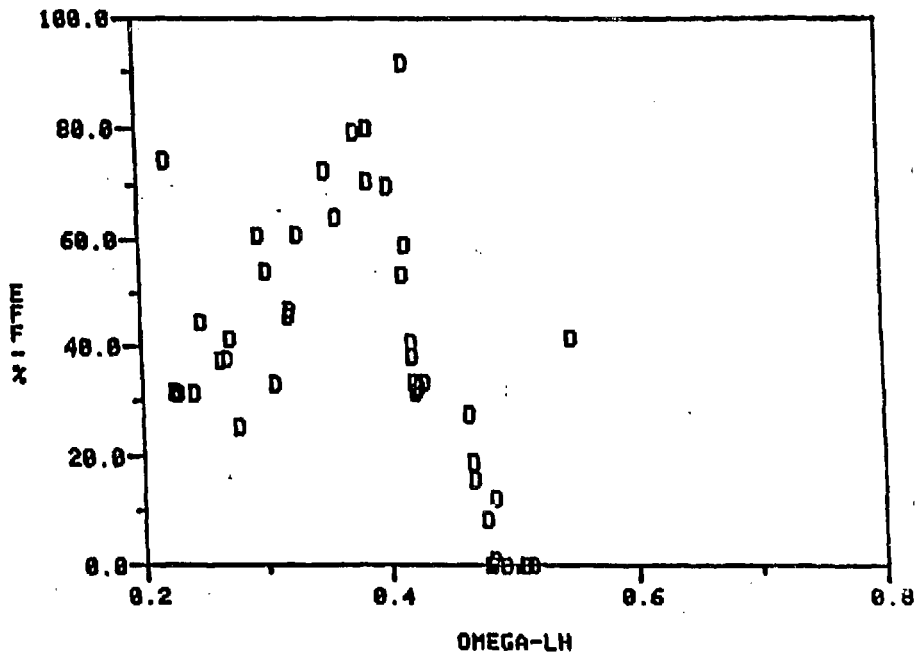
Fig. 11
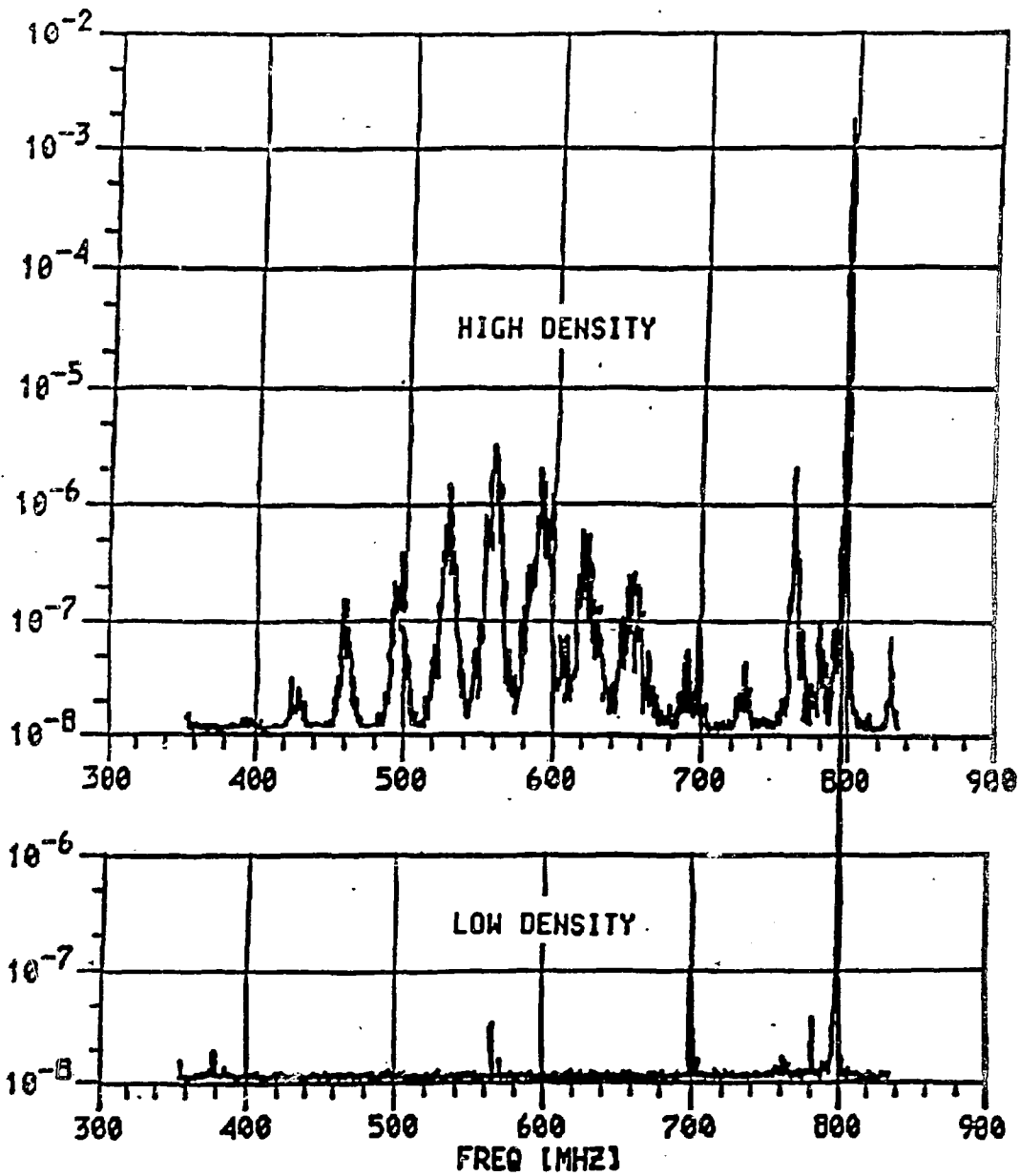
Fig. 12

Plasma Res Lab, Austra Nat'l Univ, AUSTRALIA
Dr. Frank J. Paoloni, Univ of Wollongong, AUSTRALIA
Prof. I.R. Jones, Flinders Univ., AUSTRALIA
Prof. M.H. Brennan, Univ Sydney, AUSTRALIA
Prof. F. Cap, Inst Theo Phys, AUSTRIA
Prof. Frank Verheest, Inst theoretische, BELGIUM
Dr. D. Palumbo, Dg XII Fusion Prog, BELGIUM
Ecole Royale Militaire, Lab de Phys Plasmas, BELGIUM
Dr. P.H. Sakanaka, Univ Estadual, BRAZIL
Dr. C.R. James, Univ of Alberta, CANADA
Prof. J. Teichmann, Univ of Montreal, CANADA
Dr. H.M. Skarsgard, Univ of Saskatchewan, CANADA
Prof. S.R. Sreenivasan, University of Calgary, CANADA
Prof. Tudor W. Johnston, INRS-Energie, CANADA
Dr. Hannes Barnard, Univ British Columbia, CANADA
Dr. M.P. Bachynski, MPB Technologies, Inc., CANADA
Zhengwu LI, SW Inst Physics, CHINA
Library, Tsing Hua University, CHINA
Librarian, Institute of Physics, CHINA
Inst Plasma Phys, SW Inst Physics, CHINA
Dr. Peter Lukac, Komenskeho Univ, CZECHOSLOVAKIA
The Librarian, Culham Laboratory, ENGLAND
Prof. Schatzman, Observatoire de Nice, FRANCE
J. Radet, CEN-BP6, FRANCE
AM Dupas Library, AM Dupas Library, FRANCE
Dr. Tom Mual, Academy Bibliographic, HONG KONG
Preprint Library, Cent Res Inst Phys, HUNGARY
Dr. A.K. Sundaram, Physical Research Lab, INDIA
Dr. S.K. Trehan, Panjab University, INDIA
Dr. Indra, Mohan Lal Das, Banaras Hindu Univ, INDIA
Dr. L.K. Chavda, South Gujarat Univ, INDIA
Dr. R.K. Chhajlani, Var Ruchi Marg, INDIA
P. Kaw, Physical Research Lab, INDIA
Dr. Phillip Rosenau, Israel Inst Tech, ISRAEL
Prof. S. Cuperman, Tel Aviv University, ISRAEL
Prof. G. Rostagni, Univ DI Padova, ITALY
Librarian, Int'l Ctr Theo Phys, ITALY
Miss Clella De Palo, Assoc EURATOM-CNEN, ITALY
Biblioteca, del CNR EURATOM, ITALY
Dr. H. Yamato, Toshiba Res & Dev, JAPAN
Prof. M. Yoshikawa, JAERI, Tokai Res Est, JAPAN
Prof. T. Uchida, University of Tokyo, JAPAN
Research Info Center, Nagoya University, JAPAN
Prof. Kyoji Nishikawa, Univ of Hiroshima, JAPAN
Prof. Sigeru Mori, JAERI, JAPAN
Library, Kyoto University, JAPAN
Prof. Ichiro Kawakami, Nihon Univ, JAPAN
Prof. Satoshi Itoh, Kyushu University, JAPAN
Tech Info Division, Korea Atomic Energy, KOREA
Dr. R. England, Civdad Universitaria, MEXICO
Bibliotheek, Fom-Inst Voor Plasma, NETHERLANDS
Prof. B.S. Liley, University of Waikato, NEW ZEALAND

Dr. Suresh C. Sharma, Univ of Calabar, NIGERIA
Prof. J.A.C. Cabral, Inst Superior Tech, PORTUGAL
Dr. Octavian Petrus, ALI CUZA University, ROMANIA
Dr. R. Jones, Nat'l Univ Singapore, SINGAPORE
Prof. M.A. Hellberg, University of Natal, SO AFRICA
Dr. Johan de Villiers, Atomic Energy Bd, SO AFRICA
Dr. J.A. Tagle, JEN, SPAIN
Prof. Hans Wilhelmson, Chalmers Univ Tech, SWEDEN
Dr. Lennart Stenflo, University of UMEA, SWEDEN
Library, Royal Inst Tech, SWEDEN
Dr. Erik T. Karlson, Uppsala Universitet, SWEDEN
Centre de Recherchesen, Ecole Polytech Fed, SWITZERLAND
Dr. W.L. Weise, Nat'l Bur Stand, USA
Dr. W.M. Stacey, Georg Inst Tech, USA
Dr. S.T. Wu, Univ Alabama, USA
Prof. Norman L. Oleson, Univ S Florida, USA
Bonjaml, Univ, USA
Prof. Igne Kristiansen, Texas Tech Univ, USA
Dr. Raymond Askew, Auburn Univ, USA
Dr. V.T. Tolok, Kharkov Phys Tech Ins, USSR
Dr. D.D. Ryutov, Siberian Acad Sci, USSR
Dr. M.S. Rabinovich, Lebedev Physical Inst, USSR
Dr. G.A. Eliseev, Kurchatov Institute, USSR
Dr. V.A. Glukhikh, Inst Electro-Physical, USSR
Prof. T.J. Boyd, Univ College N Wales, WALES
Dr. K. Schindler, Ruhr Universitat, W. GERMANY
Nuclear Res Estab, Julich Ltd, W. GERMANY
Librarian, Max-Planck Institut, W. GERMANY
Dr. H.J. Kaeppler, University Stuttgart, W. GERMANY
Bibliothek, Inst Plasmaforschung, W. GERMANY